Explicit formulations for advanced Green's functions with built-in boundaries

G. S. Gipson[1] & B. W. Yeigh[2]
[1]*School of Civil and Environmental Engineering, Oklahoma State University, USA*
[2]*Saint Louis University, USA*

Abstract

This paper amplifies upon a previously presented BEM formulation where the two-dimensional logarithmic fundamental solution is transformed so as to automatically accommodate rectangular boundaries with fixed boundary conditions. Explicit derivations are presented using conformal mapping. Computational examples and comparisons with the standard procedure illustrate the advantages of the method.
Keywords: Green's function, fundamental solution, boundary elements, conformal mapping, explicit formulations.

1 Introduction

In 1986, Gipson et al. [1] presented boundary element results for phreatic surface and subsurface flow using an advanced Green's function that inherently accounted for certain boundary conditions common to such analyses. Due to the nature of that presentation and space limitations in the proceedings, the details of the Green's function derivation were relegated to a reference in what has since become a difficult-to-obtain technical report [2]. In the years since the publication [1], there have been numerous requests made of the original authors to provide more substantive details of how the advanced Green's function was obtained. Also during this time, the global scope of boundary element technology has been expanded to more directly embrace the meshless methodology, which was a primary theme in the original work. This paper represents an attempt to fill the gap in the archival literature left by the omission

WIT Transactions on Modelling and Simulation, Vol 42, © 2006 WIT Press
www.witpress.com, ISSN 1743-355X (on-line)
doi:10.2495/BE06001

of the derivation, and also demonstrates how the technique can be used to accommodate other similar boundary value problems.

2 Background

Fixed rectangular boundaries with no-flux, no temperature, no displacement, etc. type boundary conditions recur frequently in practical engineering analyses. The Laplace and Poisson equations describe a wide variety of steady-state physical problems including heat transfer, electrostatics, and groundwater seepage. Terminology applicable to this latter physical application will be used here since recurrent rectangular boundaries occur so frequently in geotechnical analysis of soil-structure interaction. Examples include sheetpiles, dam structures, and U-locks. Boundary elements, because of its boundary data nature, is a natural choice for analyzing soil seepage phenomena. The domains, which theoretically are infinite half-spaces, are rarely represented as such in any analysis technique. Particularly, in finite elements, finite differences, and boundary elements, the standard procedure is to extend the mesh of analysis a *goodly distance* (using the vernacular of St. Venant) away from the region of prime interest and make an assumption about the nature of the physical phenomenon *far away.* Usually, the geotechnical engineer assumes that there is a horizontal impermeable boundary at some distance below the surface of the earth as well as vertical impermeable planes sufficiently far downstream and upstream from the region of analysis. Finite elements and finite differences both suffer from the drawback that representing the *far away* approximation typically involves the input of considerably more nodes and consequently more unknowns into the region. The size and cost of the analysis grow geometrically with the improvement in these approximate boundary conditions.

This does not happen with boundary elements. This technique is inherently superior to finite elements and finite differences in that far fewer equations and discretization effort are needed to represent the problem. Only the boundaries of the region are involved in the solution.

However, the modeling efficiency of the entire process can be improved even further, and this aspect of the general problem forms the subject of this research. The definition of the situation is best described pictorially as in fig. 1. Denote by ϕ the piezometric head which is obtained as a solution of Laplace's equation in steady-state seepage. It seems that in the synthesis of the vast majority of groundwater seepage problems, the three impermeable boundaries as described above exist in the same general configuration. These are characterized geometrically by a boundary at $y = y_{\min}$ with a no-flux boundary condition ($\partial\phi/\partial y = 0$); and two boundaries, located respectively at $x = x_{\min}$ and $x = x_{\max}$, which are also impermeable ($\partial\phi/\partial x = 0$). Since these three boundary configurations occur so frequently, it would be advantageous to eliminate the need for their explicit discretization in the boundary element representation of the problem.

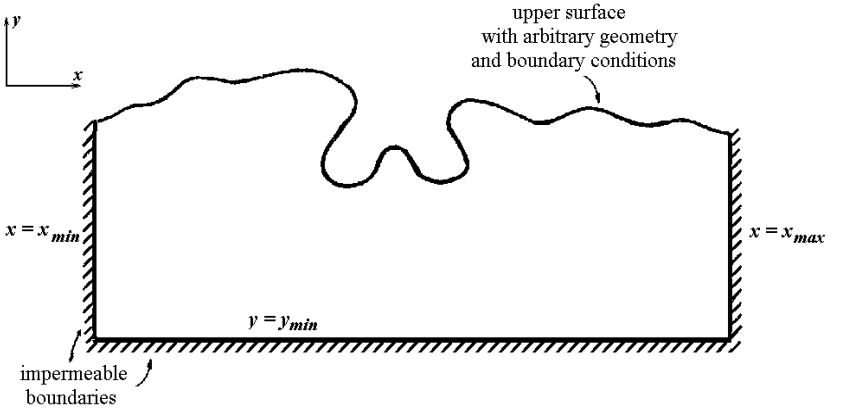

Figure 1: The basic geometrical configuration with three rectilinear, impermeable boundaries and an arbitrary upper boundary.

The way to eliminate these boundaries is to make their existence an inherent part of the mathematical formulation of the problem. In boundary elements, this is done by using an appropriate Green's function which has the no-flux conditions at certain points built-in. This is as opposed to using the free-space *fundamental solution* that is most often resorted to in boundary element methods. To the authors' knowledge, the only published Green's function for this type of problem are in references [1] and [2]. The following is a step-by-step derivation of the Green's function.

3 Derivation of the Green's function

We will assume that the homogeneous, isotropic, steady-state form of Darcy's law applies to the problem. We have

$$\frac{\partial^2 \phi}{\partial x^2} + \frac{\partial^2 \phi}{\partial y^2} = 0 \tag{1}$$

where ϕ is the total head. The Green's function ϕ^* for this problem is defined by

$$\frac{\partial^2 \phi}{\partial x^2} + \frac{\partial^2 \phi}{\partial y^2} = -\delta(x - x_0)\,\delta(y - y_0) \tag{2}$$

where $\delta(x)$ is the Dirac delta function. The physical interpretation of having a point source (sink) of unit intensity at point (x_0, y_0) is used in the definition

of ϕ^*. The fundamental solution, or equivalently, the Green's function for unbounded space is easily obtained from eqn. (2) by switching to planar polar coordinates centered at (x_0, y_0). Denote by r the radial distance from (x_0, y_0). Eqn. (2) becomes:

$$\frac{1}{r}\frac{d}{dr}\left(r\frac{d\phi^*}{dr}\right) = -\frac{\delta(r)}{2\pi r} \tag{3}$$

Two integrations yields

$$\phi^* = -\frac{1}{2\pi}\ln(r) + C_1\ln(r) + C_2$$

C_1 and C_2 may be used to fit special types of boundary conditions. They are usually unnecessary for the fundamental problem and are set to zero.
We take ϕ^* to be

$$\phi^* = -\frac{1}{2\pi}\ln(r) \tag{4}$$

a well-known result.

Although we could in principle manipulate eqn. (2) until the desired boundary conditions of fig. 1 are met, it is simpler to adapt eqn. (4) to the desired form if possible. This is can be done for a wide variety of problems using the method of images and the complex variable technique of conformal mapping. The basic premise is that the Dirichlet and Neumann problems can be solved for any simply-connected two-dimensional region which can be mapped conformally by an analytic function on to the unit circle or the half plane [3].

Denote by w the complex (u, v) plane as shown in fig. 2. If a point source with potential given by eqn. (4) is placed at (u_0, v_0), we can create a physical scenario equivalent to having an impermeable boundary along the $u-$axis. This is done by placing an image charge of the same strength at point $(u_0, -v_0)$. The new Green's function is obtained by superposing these two potentials:

$$\phi_H^* = -\frac{1}{4\pi}\ln\left[(u-u_0)^2 + (v-v_0)^2\right] - \frac{1}{4\pi}\ln\left[(u-u_0)^2 + (v+v_0)^2\right] \tag{5}$$

and the region of analysis is now reduced to a half-plane depicted in fig. 2.

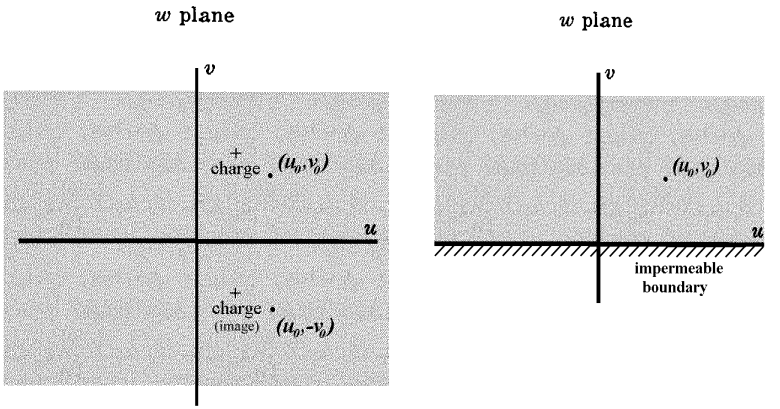

Figure 2: The entire complex plane with symmetrically placed identical point sources (left) is equivalent to a half-plane formulation (right) with an impermeable boundary at $v = 0$.

The new half-plane region may be mapped conformally into the z_1-plane (fig. 3) with

$$w = \cos\left(\frac{\pi z_1}{L}\right) \tag{6}$$

where L is an arbitrary non-zero length scale.

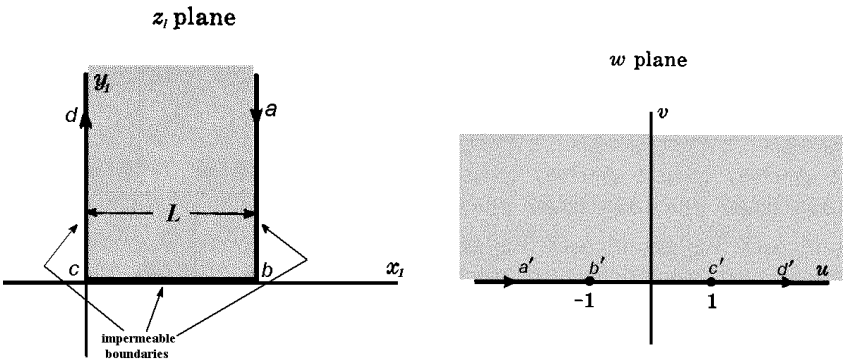

Figure 3: Mapping of the w half-plane into the z_1 plane. The boundary conditions invoked along $v = 0$ are mapped as well.

Eqn. (6) is equivalent to setting

$$\begin{aligned} u &= \sin x_1 \cosh y_1 \\ v &= \cos x_1 \sinh y_1 \end{aligned} \tag{7}$$

Note that due to the mapping, the no-flux boundary condition indicated in fig. 2 is invoked on all three finite boundaries.

The next step is to translate the entire region in the y_1 – direction such that $y = y_{\min}$ is the lower boundary, and simultaneously perform a *stretching and translation* mapping in the *x*-direction so as to fix the left and right boundaries at $x = x_{\min}$ and $x = x_{\max}$, respectively.

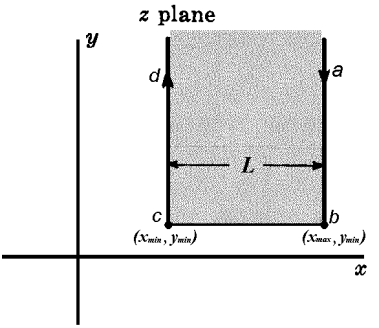

Figure 4: Mapping of the z_1 plane from fig. 3 on to the global coordinate configuration depicted in fig. 1. Note that the previously arbitrarily specified parameter *L* is now set equal to $x_{\max} - x_{\min}$.

The appropriate mapping is

$$z = x_1 + iy_1$$

with

$$x_1 = \frac{x - x_{\min}}{x_{\max} - x_{\min}} L$$
$$y_1 = y - y_{\min} \tag{8}$$

It is simplest to now set $L = x_{\max} - x_{\min}$. The mapped region is shown in fig. 4.

From eqns. (7) and (8), we have the final form of *u* and *v*:

$$u = \cos\left[\frac{\pi\left(x - x_{\min}\right)}{x_{\max} - x_{\min}}\right]\cosh\left[\frac{\pi\left(y - y_{\min}\right)}{x_{\max} - x_{\min}}\right]$$
$$v = \sin\left[\frac{\pi\left(x - x_{\min}\right)}{x_{\max} - x_{\min}}\right]\sinh\left[\frac{\pi\left(y - y_{\min}\right)}{x_{\max} - x_{\min}}\right] \tag{9}$$

and eqns.(9) are then substituted into eqn. (5) to obtain the desired Green's function. Note that the functional form appears differently than its original

appearance in Gipson et al [1] due to the use of a different mapping (sine function instead of cosine) in eqn. (6).

Once programmed into a boundary element computer code, this Green's function will allow a user to solve a groundwater flow problem (or any equivalent problem governed by Laplace's equation) by specifying boundary elements only on the upper surface, and the parameters $x_{\min}$, $x_{\max}$, and $y_{\min}$. This is a very useful result, and it has delivered perhaps the simplest possible numerical device for solving general Laplace problems of the type defined by the geometry of fig. 1.

4 Illustration

Explicit examples applicable to the seepage problem are available in reference [1]. Fig. 5, recast from that work, is an exemplary illustration to show the advantages produced by the more sophisticated Green's function. Not only does it reduce the amount of boundary element discretization considerably, but on the no-flux surfaces where no elements are required, the boundary conditions are satisfied *exactly*. Use of the advanced Green's function also reduces computational time because of the smaller number of simultaneous equations produced. In this example, 43 linear elements were used, and 44 simultaneous equations had to be solved. Equivalent accuracy with the standard fundamental solution and 77 linear elements required 78 nodes and simultaneous equations.

5 Other special Green's functions

With the conformal mapping method and other creative applications of imaging, other useful Green's functions may be produced. For instance, if the impermeable boundaries in fig. 1 are replaced with boundaries held at zero potential (the equivalent Dirichlet problem), a typical geometry that occurs in heat transfer and diffusion is the result. We may reuse all the mappings in Section 3 with the one difference that a *negative* image charge is placed at $(u_0, -v_0)$ in fig. 2 instead of positive. This renders the previous impermeable boundaries as zero-potential boundaries. The only change in the formulas occurs in eqn. (5) with a sign difference preceding the second term:

$$\phi_H^* = -\frac{1}{4\pi}\ln\left[(u-u_0)^2+(v-v_0)^2\right]+\frac{1}{4\pi}\ln\left[(u-u_0)^2+(v+v_0)^2\right] \qquad (10)$$

It should be further noted that if any portion of the implicit zero-potential is nonzero, explicit boundary elements can be placed at the location with the proper potential assigned. By the principle of superposition, the zero potential is therefore overridden.

If only two of the perpendicular boundaries are required to be held at zero potential, the configuration can be obtained by skew-reflecting the pair of

charges that produced eqn. (10) around the *v*-axis. The effect is to place positive charges at (u_0, v_0) and $(-u_0, -v_0)$, and negative charges at $(u_0, -v_0)$ and $(-u_0, v_0)$. The new Green's function follows once again from Section 3 as:

$$\phi_H^* = -\frac{1}{4\pi}\ln\left[(u-u_0)^2+(v-v_0)^2\right]+\frac{1}{4\pi}\ln\left[(u-u_0)^2+(v+v_0)^2\right]$$
$$-\frac{1}{4\pi}\ln\left[(u+u_0)^2+(v+v_0)^2\right]+\frac{1}{4\pi}\ln\left[(u+u_0)^2+(v-v_0)^2\right]$$

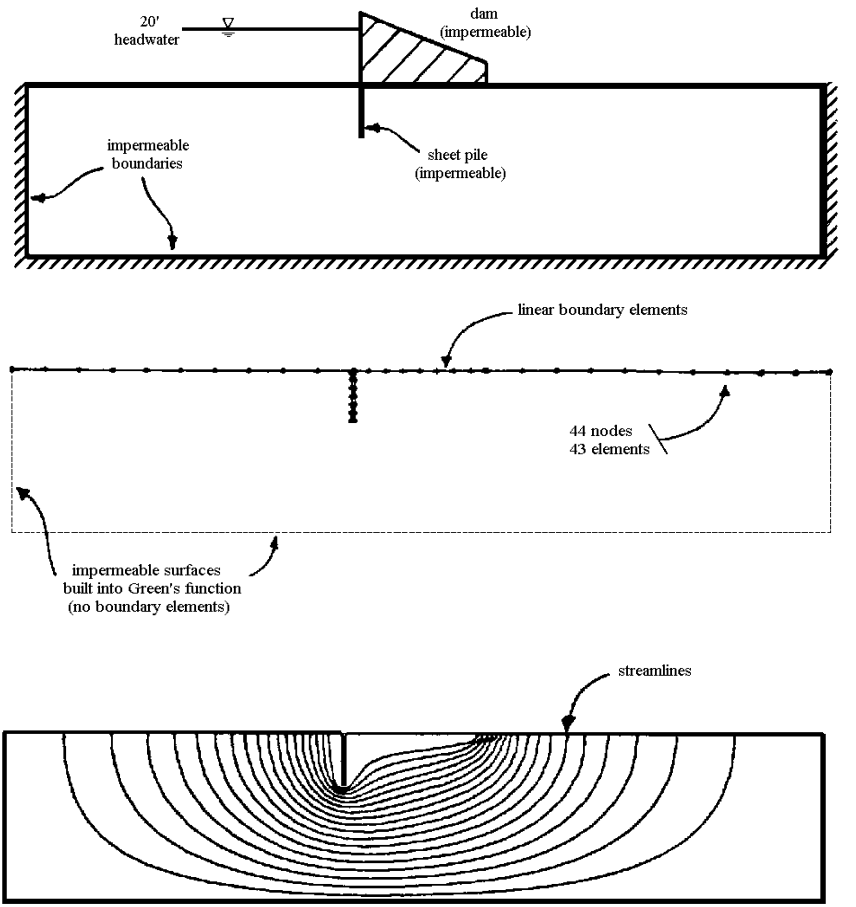

Figure 5: Boundary element analysis of a dam/sheetpile problem depicting the idealized synthesis (top), the boundary element model developed from using the advanced Green's function (middle), and the results of the analysis in the form of streamline contours (bottom).

This same idea of imaging charges and/or using conformal mapping can be continued theoretically indefinitely to produce other useful configurations for the boundary element analyst.

6 Summary and conclusions

The use of conformal mapping coupled with the method of images has been shown to produce an enhancement to the conventional boundary element method. Implicit boundaries satisfying exact boundary conditions can reduce the modeling effort and computational time while increasing the accuracy. Explicit derivations of Green's functions used in previous work have been presented. The method is a natural mesh reduction technique and can be coupled with other MRM's to further progress the efficiency of computational mechanics.

Acknowledgement

The authors would like to acknowledge the USAE Waterways Experiment Station which provided the original funding for this work.

References

[1] Gipson, G.S., Camp, C.V., Radhakrishnan, N. Phreatic surface and subsurface flow with boundary elements using an advanced Green's function. *Betech 86*, eds. J.J. Conner & C.A. Brebbia. Computational Mechanics Publications: Southampton, pp 385-94, 1986.

[2] Gipson. G.S. Applications of Boundary Elements to the Problems of the U.S. Corps of Engineers. Report to Battelle Columbus Laboratories, Contract #DAAG29-81-D-0100; 1985.

[3] Churchill. R.V., Brown, J.W., Verhey, R.F., *Complex Variables and Application 3rd ed.*, McGraw-Hill, pp. 195-238, 1974.